Progress In Electromagnetics Research C, Vol. 98, 239–255, 2020

Design and Analysis of Millimeter Wave Dielectric Resonator Antenna for 5G Wireless Communication Systems

Muhammad Anab[1, *], Muhammad Irfan Khattak[1], Syed Muhammad Owais[1], Abbas Ali Khattak[1], and Asif Sultan[2]

Abstract—Today, worldwide more than five billion of wireless devices are directly communicating for voice and data transmission. The amount of data utilization has increased remarkably and here comes 5G technology with more prominent features, offering high data rate, low latency rate, efficient EM spectrum utilization, an immense machine-2-machine communication, etc. The efficient implementation of 5G technologies requires efficient and compact antennas. This work presents a novel multiband rectangular dielectric resonator antenna for future 5G wireless communication system, having stacked radiator with semi-circular slots etched on the left and right sides of an upper radiator. Additionally, a semi-elliptical slots rectangular microstrip patch antenna of the same dimensions for the purpose of comparison is designed. 28 and 38 GHz, which are the proposed 5G bands by most researchers, are the core target of this work. Alumina with a high relative permittivity of 9.8 is used as a radiator in the design of DRA, while common in the design of both proposed antennas, Rogers RT/DUROID 5880 with a relative permittivity of 2.2 having standard thickness is used as substrate material. Both the proposed antennas have an overall same size of $13 \times 11.25\,\text{mm}^2$. The proposed dielectric antenna resonates at 25.4, 34.6 and 38 GHz with 7.34, 4.04, and 3.30 GHz of wide impedance bandwidth covering the targeted 5G, 28, and 38 GHz bands, having a good return loss of -34.7, -31.8, and -33.5 dB, respectively. Further, the proposed dielectric antenna has a maximum radiation efficiency of 97.63%, with overall radiation efficiency greater than 90%, and maximum gain of 7.6 dBi is also noted. On the other hand, the proposed microstrip antenna resonates at 28 and 38 GHz with a 1.49 and 1.01 GHz of moderate impedance bandwidth, having -23.6 and -27.1 dB of satisfactory return loss. Further, the proposed patch antenna has a maximum radiation efficiency of 90.33% at 28 GHz, with overall radiation efficiency of greater than 84%, and moderate gain of 5.45 dBi is also noted. Both the proposed antennas have a nearly omnidirectional radiation pattern at resonance frequencies, with VSWR less than 2. Comparative study of the two proposed antennas regarding radiation efficiency, return loss, gain, data rate, and impedance bandwidth evidently shows that performance of DRA over MPA at millimeter wave is very good. The proposed antennas are simulated in CST Microwave studio v18.

1. INTRODUCTION

The productive and efficient usage of information and communication technologies (ICT) is proving useful, in improving the economy of the world [1]. Wireless communication networks are possibly the most crucial factor in world ICT strategy, supporting many other industries. It is one of the fastest emerging and most vivid and dynamic areas in the world [2]. The development of wireless communication technologies has remarkably changed people's lifestyle in terms of communication, business, and social functions.

Received 24 October 2019, Accepted 23 December 2019, Scheduled 10 January 2020

* Corresponding author: Muhammad Anab (m.anab@uetpeshawar.edu.pk).

[1] Department of Electrical Engineering, University of Engineering & Technology, Peshawar, Pakistan. [2] Senior Engineer Pakistan Telecom Company Limited, Pakistan.

The remarkable success of wireless communication technologies can be imagined by the dramatic growth of technology innovation. Cellular wireless communication industry has experienced a rapid development, i.e., it progresses from analog 1G (AMPS) to digital 2G (GSM), then to high data rate 3G (WCDMA), 3.5G (HSPA), and 4G (LTE and LTE advanced) cellular wireless communication systems [3]. The 4G cellular wireless communication systems have been launched in most of the countries. In spite of that, with an upsurge of wireless devices and services, there are still some problems and challenges that cannot be solved even by 4G, like high energy consumption and spectrum crisis [4]. With increasing demand for efficient wireless services, spectrum deficiency is one of the challenging factors in today's wireless communication industries. To cope with it, the use of millimeter wave bands (20–300 GHz), which have huge amount of bandwidth for higher data rate transmission, becomes necessary. Millimeter wave bands, which are considered to be an important part of future 5G cellular network, have been proposed to provide multi-gigabit wireless communication services like ultra-high definition video (UHDV) and high definition television (HDTV) [5]. There are different bands proposed for future 5G, and among them, 28 GHz is one of the bands [6–9]. The proposed prime spectrum for 5G application is 20–90 GHz [10]. It has been found that millions of wireless devices will communicate with each other using 5G technologies and will enjoy a huge data rate of 1 to 10 Gbps (theoretically). Various future visions technologies that will come into existence due to 5G technology are: Smart grids, Smart cities, Virtual reality, Machine to machine communication, Autonomous driving, Telemedicine, etc.

Whatever the advancement made by new release wireless technologies, the aim of every wireless technology is to collect data, which is not possible without an antenna, so an antenna plays a basic role and can affect the whole system functions in terms of bandwidth, beamwidth and efficiency. With the rapid development in wireless communication system, the need for improved characteristics antenna design such as antenna size, traffic demand, high data rate, bandwidth, gain, and efficiency, increases. These required features lead to various antenna designs to achieve tradeoffs in antenna size vs antenna cost, high radiation efficiency and high gain vs low loss, high bandwidth, and high data rate [11–18]. Numerous microstrip antennas have been designed for various applications, i.e., for WLAN, PCS, 2G, 3G, and for 4G [19–22].

Various microstrip antenna designs have been proposed for future 5G wireless communication network. In [23], an antenna with coplanar feeding of size $5 \times 5\,\text{mm}^2$, Rogers RT5880 substrate of thickness 0.254 mm, having 6.6 dB gain at 28 GHz is proposed. In [24], an antenna resonating on 60 GHz frequency having gain of 5.48 dB using H-slot and E-slot is proposed. Some works have been recently released [25–27] by different authors on designing 5G antennas/arrays.

Highly effective antennas, which bear high radiation efficiency, high gain, high temperature stability, etc., are needed for high frequencies (mm) applications (5G), but the performances of conventional microstrip patch antennas and Vivaldi antennas are limited in terms of radiation efficiency, gain, etc., by the severe metallic (ohmic) losses at high frequencies. Consequently, an alternate and novel antenna technology known as Dielectric Resonator Antenna having a ceramic dielectric radiator made up of low loss dielectric material of different geometries like rectangle, hemisphere, cylinder, ring, etc. [28], instead of conducting radiator (patch) was developed and investigated by antenna researchers in late nineteen eighties. Because of the freedom form conduction losses, dielectric antennas show better performance than MPA with reference to radiation efficiency, return loss, temperature stability, gain, data rate, and impedance bandwidth. The advantages of dielectric antennas over patch antennas include wider impedance bandwidth, wide control over bandwidth as bandwidth of DRA depends on relative permittivity and attributes (length, width etc.) of its radiator, wide control over size as size of DRA inversely varies with the dielectric constant of its radiator, high radiation efficiency as freedom from inherited ohmic losses and negligible surface waves, higher power and temperature handling ability as of ceramic dielectric materials of temperature stable and high dielectric strength, high polarization clarity, high gain mainly at high frequencies as having no conduction losses and negligible spurious feed radiation, etc.

Various dielectric antenna designs prior to 5G technology have been reported, like in [29] a compact and dual-band dielectric resonator antenna operating at 880–960 MHz and 1700–2700 MHz having 80 MHz and 1 GHz bandwidths, using multibranch monopole feeding technique for mobile terminals covering Digital Communication System (DCS), Personal Communication System (PCS), Global System

for Mobile (GSM), Universal Mobile Telecommunication System (UMTS), and Long Term Evaluation (LTE) cellular bands. In [30], a multiband dielectric resonator antenna, possessing rectangular geometry, operating at 1.8, 2.2, and 2.6 GHz having 80, 30, and 200 MHz impedance bandwidths, with 6.41, 6.9, and 7.1 dBi gains, respectively, covering GSM1800, DVB-SH, and LTE-A cellular bands, is proposed. A single band two ports MIMO DRA, possessing rectangular shape operating at 2.6 GHz LTE band with different permittivity dielectric materials, used for size reduction, excited by slot microstrip and coaxial probe, is presented in [31]. Size of the proposed LTE antenna design [31] for dielectric material of permittivity 10 is $46 \times 28 \times 15\,\text{mm}^3$ with ground plane of $65 \times 45\,\text{mm}^2$, and reduced size with permittivity 30 is $15 \times 24 \times 10\,\text{mm}^3$ having ground plane of $45 \times 25\,\text{mm}^2$.

Numerous 5G single band dielectric resonator antenna designs have been found in literature. Like in [32], a complex hybrid multilayer single band dielectric resonator antenna design, excited by Substrate Integrated Waveguide (SIW) feeding technique, operating from 62 to 78 GHz with 16 GHz of wide impedance bandwidth having a 9.9 dBi of maximum gain with a small variation of 0.3 dBi in gain, is presented. Two different substrate materials are arranged into four layers, having different dimensions of 0.381, 0.381, 0.508, and 0.254 mm, in which layers 1, 2, and 3 are Rogers 5880 while layer 4 is Rogers 6010 with a relative permittivity of 2.2 and 10.2, respectively. 18 µm copper layers are printed on either side of substrates 1 and 2, whereas there are silicon glass adhesions among substrates 3 and 4 and substrates 2 and 3 [33]. A four-port single band cylindrical MIMO DRA excited by SIW feeding method, operating at 5G band 27.7 GHz with 1.91 GHz of acceptable impedance bandwidth having -30 dB of S_{11} and bearing a maximum gain variation from 5.07 to 5.70 dBi, is presented. In [34], a wideband dielectric resonator antenna, operating from 6.23 GHz to 11.4 GHz with 5.5 GHz (58%) of wide impedance bandwidth fed by coaxial probe feeding mechanism and bearing 5.4 dBi of maximum gain, having H-shape resonator of dielectric material of permittivity 30 of dimensions $10 \times 5.7 \times 2\,\text{mm}^3$, is designed. Some works have recently been released [35–42], by different researchers on designing 5G dielectric antennas operating at single band, 60 GHz.

A lonely dual-band dielectric resonator antenna operating at 10.5 and 17 GHz 5G bands, having vertically stacked rectangular dielectric radiator of AR1000 dielectric material of high relative permittivity of 9.8, excited through tilted elliptical slot aperture coupled microstrip line feeding mechanism is presented in [43]. The proposed design possesses overall size of $48 \times 40\,\text{mm}^2$ with 5.7 and 6.9 dBi maximum gains at 10.5 and 17 GHz, respectively.

Till now, no such a compact size novel multiband dielectric resonator antenna with outstanding results, proposed in this work for future 5G communication system, has been reported in literature. This work presents a novel multiband rectangular dielectric resonator antenna for a future 5G wireless communication system, having stacked radiator with semi-circular slots etched on the left and right sides of upper radiator. Additionally, a semi-elliptical slots rectangular microstrip patch antenna of the same dimensions for the purpose of comparison is designed. 5G bands, 28 and 38 GHz which are the proposed 5G bands by most researchers, are the core target of this work.

Designs of the proposed antennas are described in Section 2 in detail, whereas Section 3 covers the parametric analysis of the proposed designs. In Section 4, detailed results of the proposed designs are discussed, and Section 5 concludes the proposed work.

2. ANTENNA DESIGN AND THEORY

As this research article comprises two different antenna designs, the design procedure of each antenna is explained individually below in subsections.

2.1. DRA Design

The basic structure of DRA mainly consists of a dielectric radiator on top, a substrate of dielectric material, conducting ground, and a feed line. So, the proposed design has almost the same composition except that a vertically stacked dielectric radiator is used as can be justified from the final geometry and exploded view illustrated in Figures 1(a) and (b), respectively. Perspective and back views are shown in the next figure (Figures 2(a) and (b)). Also, performance and resonant modes of the DRA are greatly affected by the choice of the geometry and dielectric constant of the radiator used. Due

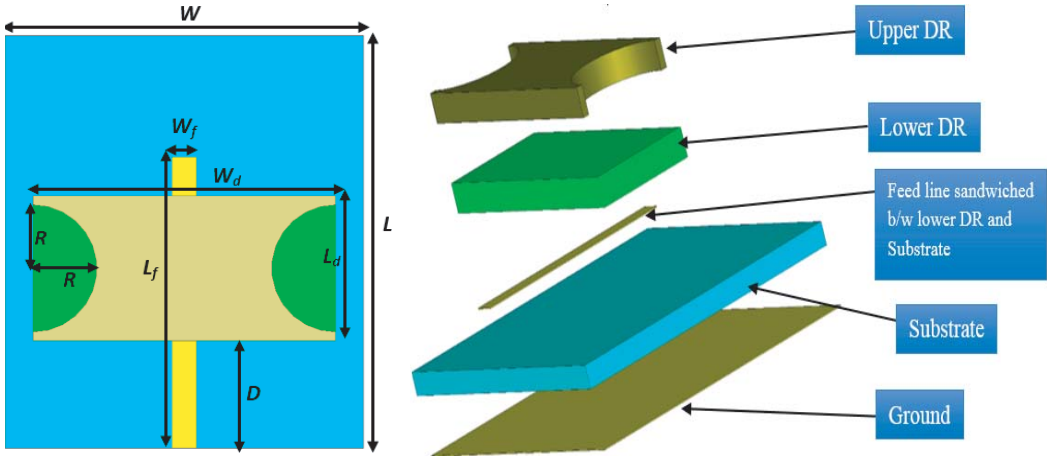

Figure 1. (a) Final geometry and (b) exploded view of proposed rectangular dielectric antenna.

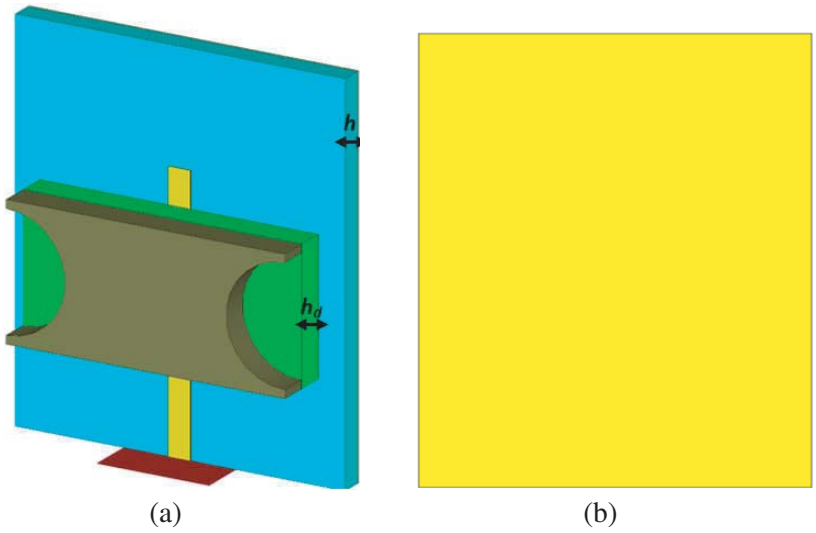

Figure 2. (a) Perspective and (b) rear view of proposed rectangular dielectric antenna.

to the design flexibility of rectangular shape geometry having three different independent physical parameters, i.e., length, width, and height, resonance frequency and bandwidth of DRA can be easily controlled. Therefore, considering its various advantages, a rectangular shape dielectric radiator (DR) of size $4.566 \times 9.5\,\text{mm}^2$, made up of ceramic material Alumina having high relative permittivity of $\varepsilon_r = 9.4$ with low tangent loss of 0.0004 of thickness of 1 mm is used. The proposed design has compact size of $13 \times 11.25\,\text{mm}^2$ having Rogers RT5880 substrate material of dielectric constant $\varepsilon_r = 2.2$ with low tangent loss of 0.0009. Standard thickness of 0.787 mm is used for substrate material with the dimensions of $13 \times 11.25 \times 0.787\,\text{mm}^3$. Copper having standard thickness of 0.035 mm is used for ground and feed line, whereas the dimensions of ground are almost same as that of substrate except height ($13 \times 11.25 \times 0.035\,\text{mm}^3$).

As the proposed RDRA is mainly composed of vertically stacked radiators, the length and width of the two radiators are same, i.e., $4.566 \times 9.5\,\text{mm}^2$, whereas a semicircular slot of radius 2 mm is etched on left and right sides of the upper radiator, as can be illustrated from Figure 1(a). Microstrip feed line (m-line), upon which the dielectric radiators are placed directly at -0.83 mm away from centered point of substrate, having $9.17 \times 0.77 \times 0.035\,\text{mm}^3$ of overall size, is the adopted feeding method. The final parameters are summarized in Table 1.

Table 1. Final parameters value of proposed RDRA.

Parameter	Value (mm)	Parameter	Value (mm)
L	13	W	11.25
L_d	4.566	W_d	9.5
L_f	9.17	W_f	0.77
R	2	M_t	0.035
H	0.787	h_d	1
D	3.387		

L = length of Substrate/Ground; W = width of Substrate/Ground; H = thickness of Substrate; L_d = length of single DR; W_d = width of single DR; h_d = height of single DR; L_f = length of feed line; W_f = width of feed line; Mt = height of ground/feed line; R = Radius of circular slot; D = distance between DR and Substrate;

By means of Dielectric Waveguide Model (DVM), resonant frequency of Transverse Electric (TE) mode of rectangular dielectric antennas can be calculated [44]. Respective formulas used for the calculation of the resonance frequency f_r of proposed dielectric antenna having rectangular radiator of dielectric constant ε_r mounted on ground plane are stated below and are given in [45];

$$f_r = \frac{c}{2\pi\sqrt{\varepsilon_r}}\sqrt{k_x^2 + k_y^2 + k_z^2} \tag{1}$$

where $k_x = \frac{\pi}{a}$, $k_z = \frac{\pi}{2b}$, $d = \frac{2}{k_y}\tanh(\frac{k_{y0}}{k_y})$, $k_{y0} = \sqrt{k_x^2 + k_z^2}$.

In Equation (1), C is equal to 3×10^8 m/sec and is the speed of light in free space, while a, b, and d denote physical parameter length, height, and width of the rectangular radiator, respectively.

The final structure shown in Figure 1(a) is achieved through the stepwise evolution of the rectangular shape radiator by using stacking approach and etching slots. Initially, a single rectangular radiator of dimensions calculated according to Equation (1) is designed, as shown in Figure 3(a). In next step, another rectangular radiator of same dimensions is stacked over the first one (see Figure 3(b)). In the third step, semicircular slots are produced in upper radiator in both left and right corners (see Figure 3(c)). Finally, both the radiators are translated along feed line from centered point towards negative y-axis (-0.83 mm), as shown in Figure 3(d).

The effect of each iteration on S_{11} is shown in the same figure (Figure 3(e)). Initially with single DR (Ant1), antenna resonates at two different bands while covering the calculated resonance frequency, 29.04–33.54 GHz and 36.2–40 GHz, with impedance bandwidths of 4.5 and 3.8 GHz, respectively. Next with stacked DR (Ant2), antenna resonates at the two bands but with much improved bandwidth which

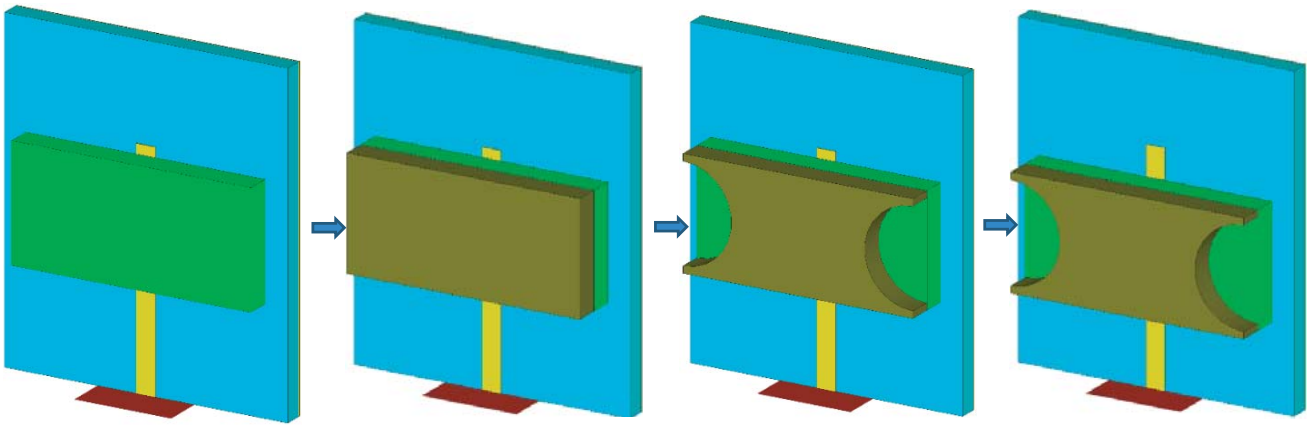

(a) (b) (c) (d)

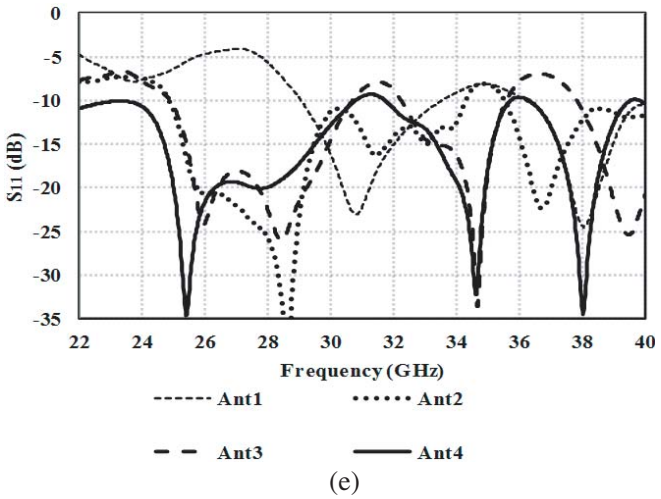

(e)

Figure 3. Structural evolution of proposed rectangular dielectric antenna. (a) Ant1: Single DR, (b) Ant2: Stacked DR, (c) Ant3: Semicircular slots etched in upper DR, (d) Ant4: DRs translated from centered point and (e) effect of each iteration on S_{11} (dB).

is the sole purpose of stacking phenomena; 25–34.5 GHz with 9.5 GHz wide bandwidth and second band starts form 35.5 GHz and continues beyond 40 GHz. In the third iteration, with semicircular slots (Ant3) etched for the purpose of multiband operation, antenna resonates at three different bands, 25–30.8 GHz, 32.2–35.5 GHz with 5.8 and 3.3 GHz impedance bandwidths, respectively, and the last band starts from 37.9 GHz and continues beyond 40 GHz. Finally, with translating both radiators along feed line from centered point towards negative y-axis (Ant4), amazing changes can be observed in the results; antenna resonates at three bands covering 28, 35, and 38 GHz 5G bands with 7.34, 4.04, and 3.30 GHz wide impedance bandwidths.

2.2. MPA Design

In the second part of the proposed work, MPA of the identical shape and dimension ($13 \times 11.25\,\text{mm}^2$) with a semielliptical slot printed on either sides of radiator (patch) is designed for the purpose of comparability, using the same substrate (Rogers RT5880) with same dimensions ($13 \times 11.25 \times 0.787\,\text{mm}^3$)

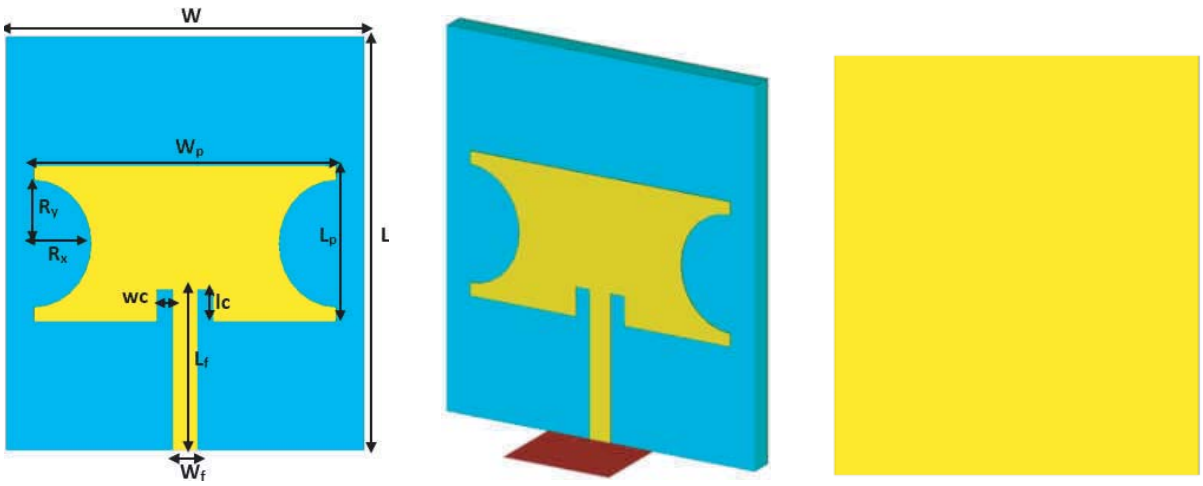

(a) (b) (c)

Figure 4. (a) Final geometry, (b) perspective and (c) rear view of proposed rectangular patch antenna.

used for the design of proposed RDRA as can be justified from the final geometry illustrated in Figure 4(a). Perspective and back views are shown in the figure (Figures 4(b) and (c)). A rectangular radiating patch of dimensions $4.9 \times 9.5 \times 0.035\,\text{mm}^3$ is printed on a substrate with semielliptical slots of radii, $1.8\,\text{mm} \times 2\,\text{mm}$ (radii along x and y-axes) produced on its either sides along width, for the purpose of increasing antenna electrical length and multiband operation. Microstrip line inset feed having size of $5.05 \times 0.77 \times 0.035\,\text{mm}^3$ is the adopted feeding mechanism. $1 \times 0.5\,\text{mm}^2$ is the dimensions of inset cut. The final parameters are summarized in Table 2.

Table 2. Final parameters value of proposed RMPA.

Parameter	Value (mm)	Parameter	Value (mm)
L	13	W	11.25
L_p	4.9	W_p	9.5
L_f	5.3	W_f	0.77
R	1.8	R_y	2
M_t	0.035	H	0.787
W_c	0.5	L_c	1

L = length of Substrate/Ground; W = width of Substrate/Ground; H = thickness of Substrate; L_p = length of radiating patch; W_p = width of radiating patch; L_f = length of feed line; W_f = width of feed line; Mt = height of patch/ground/feed line; R_x = shorter radius of elliptical slot along x-axis; R_y = longer radius of elliptical slot along y-axis; W_c = width of inset cut; L_c = length of inset cut.

3. PARAMETRIC STUDY

This section contains the parametric study to achieve the optimum design value for the proposed antennas. In order to emphasize the necessity of the stacked DRA having semicircular slot and dual-band MPA having semielliptical slot, parametric studies are conducted. There are a number of parameters that have an important effect on the performance of the antenna like length and width of radiating element, radii of the circular and elliptical slots, etc. used in the designing of the proposed antennas. A variation in the impedance bandwidth of the antenna is analyzed with respect to the parameters mentioned above.

Variations in impedance bandwidth and S_{11} of the proposed dielectric antenna with respect to length and width of rectangular radiator (dielectric), radius of semicircular slot, and position of DR on feed line are summarized in Figures 5(a), (b), (c), and (d)). With increasing the length of radiator, shift towards left can be observed in the resonance frequency (see Figure 5(a)), whereas slight shift towards left can be observed by increasing the width of radiator (see Figure 5(b)). Further by increasing the radius

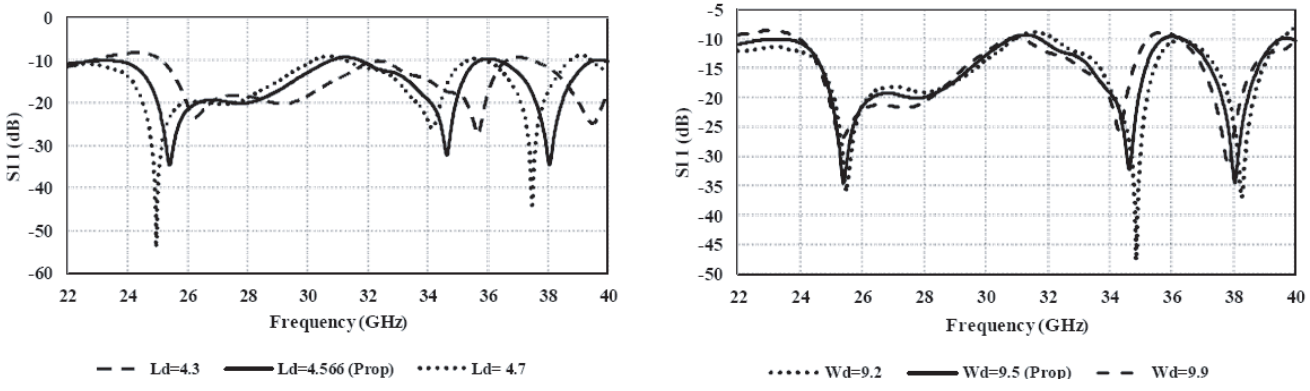

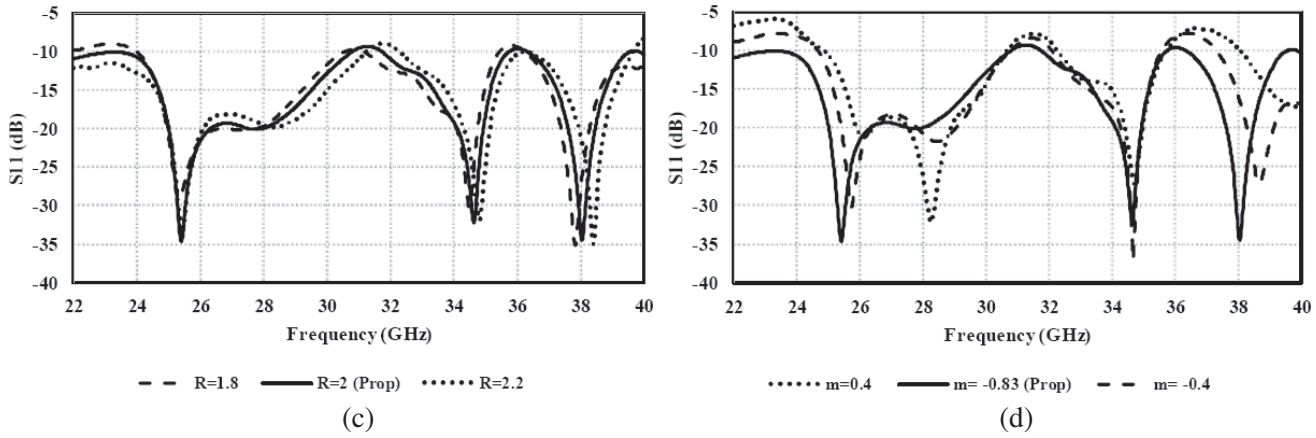

Figure 5. Variation in impedance bandwidth and S_{11} of proposed rectangular dielectric antenna w.r.t (a) length of DR, (b) width of DR, (c) radius of semicircular slot etched in upper radiator and (d) position of stacked DR on feed line.

of semicircular slots, slight shift towards higher frequencies (right) occurs at resonance frequencies 34.6 and 38 GHz, with almost negligible impact at 28 GHz, which is shown in Figure 5(c). Finally, impedance bandwidth and S_{11} are greatly affected at resonance frequencies 28 and 38 GHz by varying the position of dielectric radiator along feed line from positive axis toward negative axis, with almost no impact at

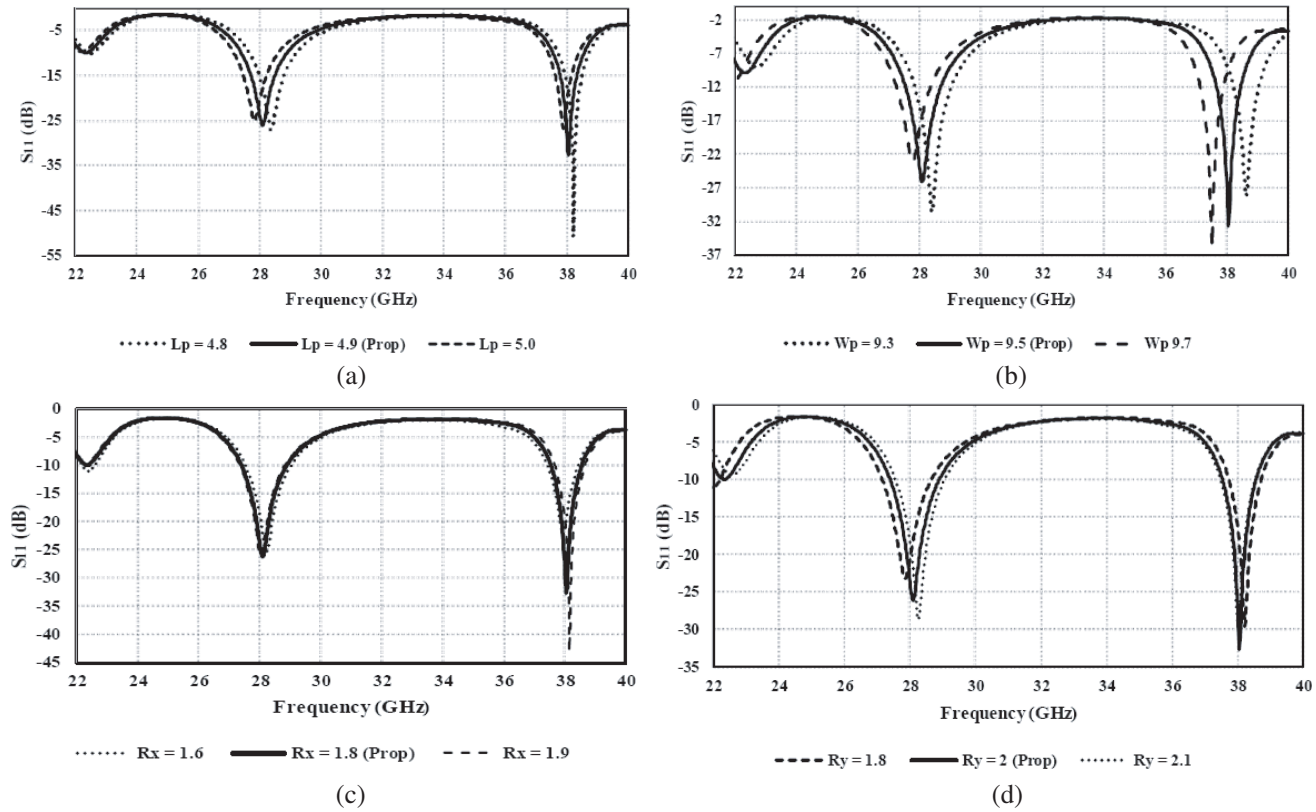

Figure 6. Variation in impedance bandwidth and S_{11} of proposed rectangular patch antenna w.r.t (a) length of patch, (b) width of patch, (c) radius of semielliptical slots along x-axis and (d) radius of Semielliptical slots along y-axis.

34.6 GHz, as can be seen in Figure 5(d). The best results are obtained when the stacked DR of length 4.566 mm, width 9.5 mm with a semicircular slot of radius 2 mm are placed below the origin at 0.83 mm.

On the other hand, variations in impedance bandwidth and S_{11} of the proposed patch antenna with respect to length and width of rectangular radiator (patch), radii of semielliptical slots along x and y-axis are summarized in Figures 6(a), (b), (c), and (d)). With increasing the length of patch, shift towards left can be observed in the resonance frequency (see Figure 6(a)), whereas slight shift towards left can be observed by increasing the width of patch (see Figure 6(b)). Further by increasing the radius of semielliptical slots along x-axis (R_x), slight shift towards right occurs at resonance frequency 38 GHz, with almost negligible impact at 28 GHz, which is shown in Figure 6(c). Finally, with increasing radius of semielliptical slots along y-axis (R_y), slight shift towards right occurs at resonance frequency 28 GHz, while slight shift towards left can be observed at 38 GHz, with almost no change in their return loss (see Figure 6(d)). The best results are obtained when the rectangular patch of length 4.9 mm, width 9.5 mm with semielliptical slots of radii 1.8 and 2 mm along x and y-axes are used.

4. RESULTS

Photographic image of the front and back of the fabricated proposed dielectric antenna validating the proposed simulated design can be seen in Figures 7(a) and (b). The proposed dielectric antenna is capable of operating at 5G bands as can be justified from the graph of return loss (S_{11}) shown in Figure 8(a). The antenna resonates at 25.4, 34.6, and 38 GHz covering 5G targeted bands, 28 and 38 GHz with a wide impedance bandwidth of 7.34, 4.04, and 3.30 GHz, respectively. A good return loss of -34.7, -31.8, and -33.47 dB at resonance frequencies 25.4, 34.6, and 38 GHz, respectively, can be observed, while an acceptable return loss of -19.96 can be observed at operating frequency 28 GHz. The VSWRs of the proposed dielectric antenna at resonance frequencies are 1.03, 1.05, and 1.043 as depicted in Figure 8(b). Simulated return loss and VSWR can be corroborated from the measured return loss and VSWR, shown in Figure 8.

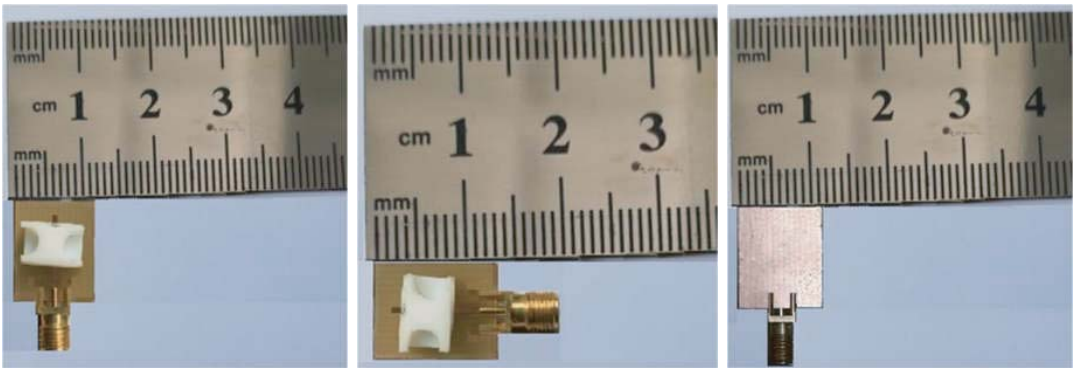

(a) (b)

Figure 7. Photographic image of (a) front and (b) back of the fabricated rectangular dielectric antenna.

The proposed dielectric antenna has a 7.6 dBi of high simulated gain at 29.2 GHz which is the operating frequency as can be seen in Figure 9(a), whereas the simulated gains at resonance frequencies are also pretty good, i.e., 6.4, 5.88, and 7.04 dBi at 25.4, 34.6, and 38 GHz, respectively. The graph of directivity (dBi) is also shown in Figure 9(a). As there is very close relation between the gain and directivity shown above, the proposed dielectric antenna possesses maximum radiation efficiency of overall greater than 90% at operating (see Figure 9(b)). Simulated gain, directivity, and radiation efficiency can be corroborated from the measured gain, directivity, and radiation efficiency, shown in Figures 9(a) and (b).

The proposed dielectric antenna possesses somehow omnidirectional radiation pattern in both principal planes, except the E-plane at 25.4 GHz which has partial directional radiation pattern. The

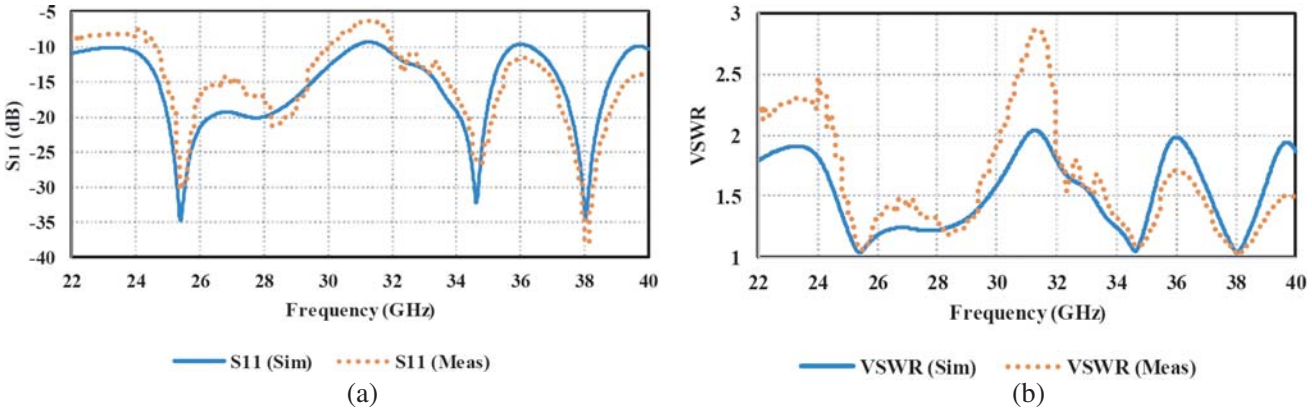

Figure 8. Simulated and Measured (a) S_{11} and (b) VSWR of the proposed rectangular dielectric antenna.

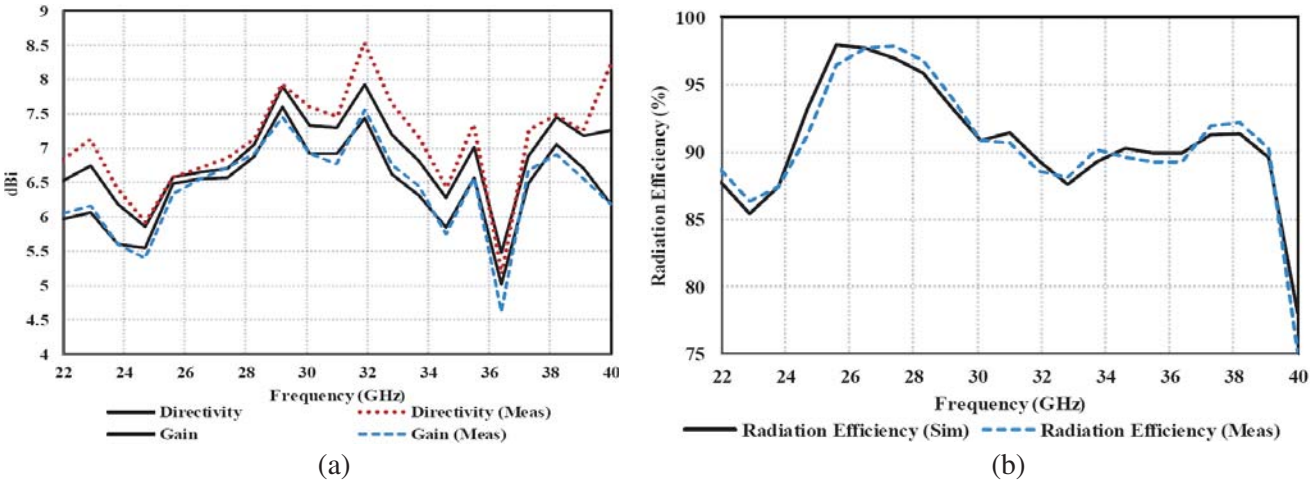

Figure 9. Proposed rectangular dielectric antenna simulated and measured (a) gain, directivity and (b) radiation efficiency.

simulated and measured omnidirectional radiation patterns in both planes at 28, 34.6, and 38 GHz, whereas the partial radiation pattern in E-plane and nearly omnidirectional pattern in H-plane at 25.5 GHz are illustrated in Figures 10(a), (b), (c), and (d). 3D gain plots at aforementioned frequencies are also illustrated in Figures 11(a), (b), (c), and (d).

Photographic image of the front and back of the fabricated proposed patch antenna validating the proposed simulated design can be seen in Figures 12(a) and (b). The proposed patch antenna is capable of operating at 5G 28 and 38 GHz bands as can be justified from the graph of return loss (S_{11}) shown in Figure 13(a). An acceptable return loss of -23.6 and -27.1 dB with 1.49 and 1.01 GHz impedance bandwidths can be observed at resonance frequencies, 28 and 38 GHz, respectively. The VSWRs of the proposed dual-band patch antenna at resonance frequencies are 1.14 and 1.09 as depicted in Figure 13(b). Simulated return loss and VSWR can be corroborated from the measured return loss and VSWR, shown below.

The proposed patch antenna has 5.45 dBi of high simulated gain at 28.88 GHz which is the operating frequency as can be seen in Figure 14(a), whereas the simulated gains at resonance frequencies 28 and 38 GHz are 5.41 and 4.89, respectively. The graph of directivity (dBi) is also shown in Figure 14(a). As there is somehow difference between the gain and directivity shown in Figure 14(a), especially at 38 GHz, the proposed dual-band patch antenna possesses maximum radiation efficiency greater than

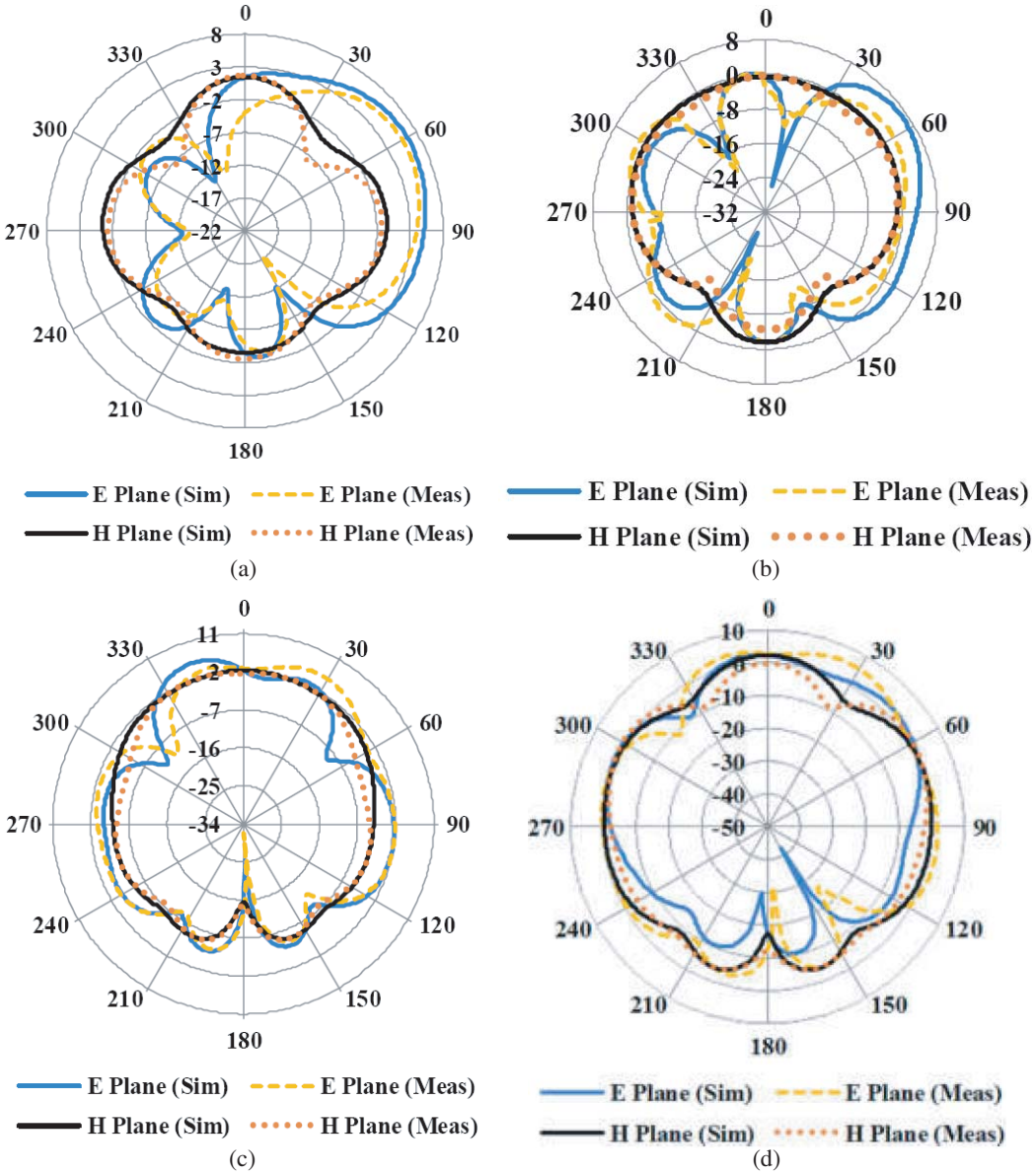

Figure 10. Simulated and measured radiation pattern in E and H-plane at (a) 25.4 GHz, (b) 28 GHz, (c) 34.6 GHz and (d) 38 GHz of the proposed rectangular dielectric antenna.

84% at operating (see Figure 14(b)), whereas 90.33% and 84.32% of moderate radiation efficiencies at 28 and 38 GHz, respectively, can also be seen. Simulated gain, directivity, and radiation efficiency can be corroborated from the measured gain, directivity, and radiation efficiency, shown in Figures 14(a) and (b).

The proposed patch antenna possesses nearly omnidirectional radiation pattern in both principal planes. The simulated and measured radiation patterns are omnidirectional in both planes (E and H-planes) at 28 and 38 GHz, illustrated in Figures 15(a) and (b). 3D gain plots at aforementioned frequencies are also illustrated in Figures 16(a) and (b).

4.1. Comparative Analysis

Comparative study of both the proposed antennas regarding radiation efficiency, return loss, gain, data rate, and impedance bandwidth is summarized in Table 3, which evidently shows that the performance

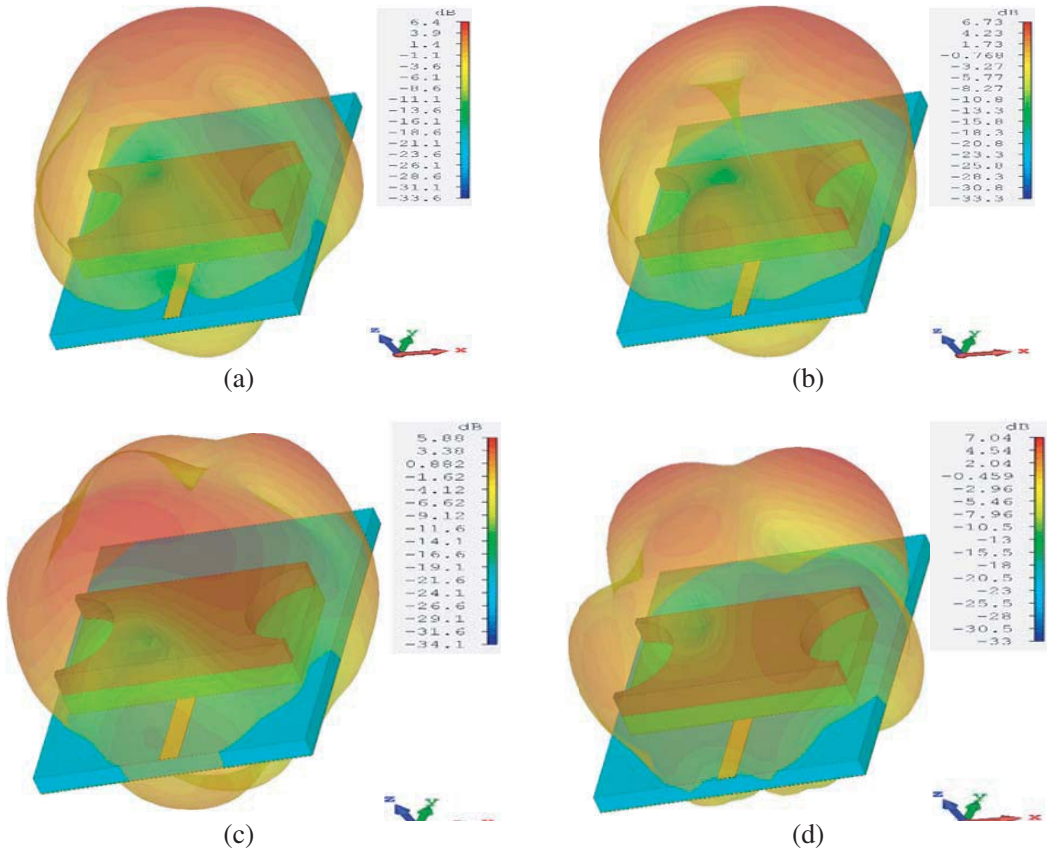

Figure 11. 3D view of gain plots at (a) 25.4 GHz, (b) 28 GHz, (c) 34.6 GHz and (d) 38 GHz of the proposed rectangular dielectric antenna.

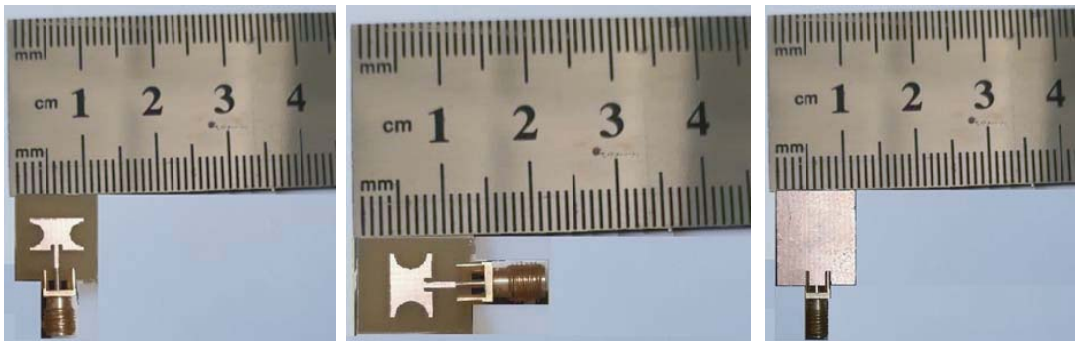

Figure 12. Photographic image of (a) front and (b) back of the fabricated rectangular dual band patch antenna.

of DRA over MPA at millimeter wave is very good, which validates the theoretical statement, due to freedom form metallic (conduction) losses, and the dielectric antenna shows better performance than its counterpart patch antennas. Comparative analysis is mainly focused on 28 and 38 GHz bands. It should be noted that the data rate shown in Tables 3 is considered using Nyquist Bit Rate equation given below, while taking single level (L) of value 2;

$$Bit\ Rate = 2 \times Bandwidth\ \times \log_2 L$$

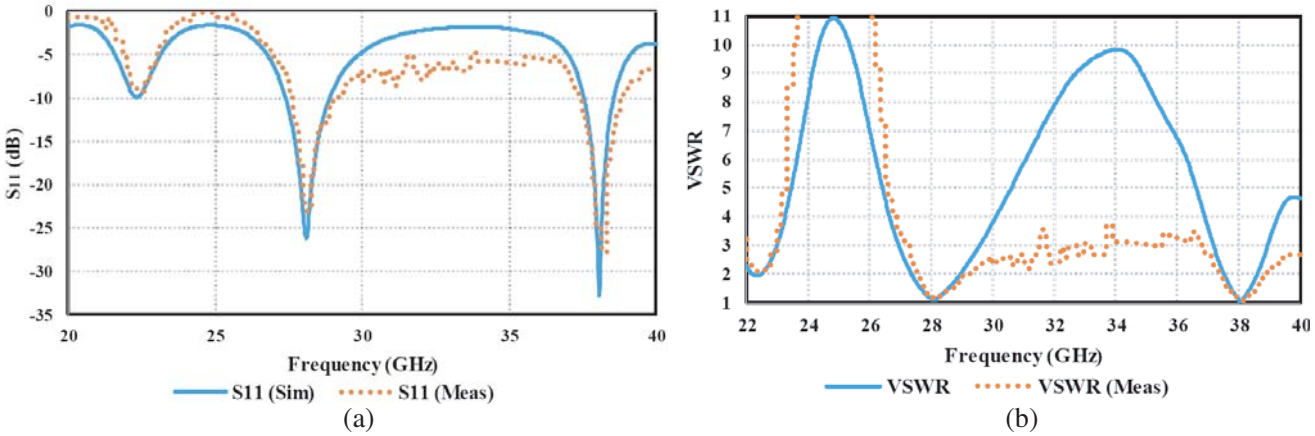

Figure 13. Simulated and measured (a) S_{11} and (b) VSWR of the proposed rectangular dual band patch antenna.

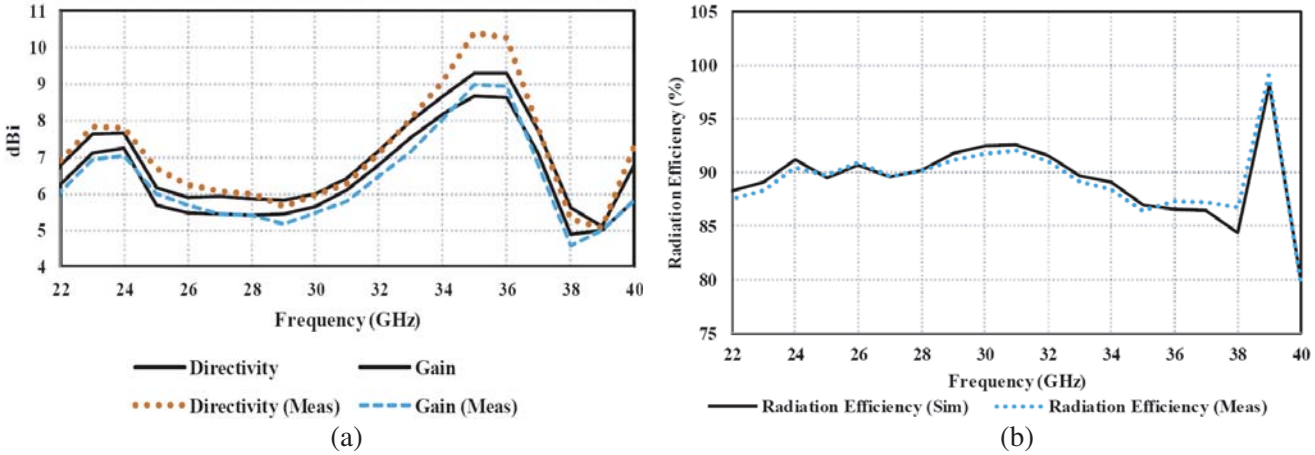

Figure 14. Proposed rectangular dual band patch antenna simulated and measured (a) gain, directivity and (b) radiation efficiency.

Table 3. Comparison of proposed rectangular dielectric antenna over rectangular dual band patch antenna.

Characteristics	Operating Frequency (GHz)	Impedance Bandwidth (GHz)	Return Loss (S_{11} dB)	VSWR	Gain (dB)	Radiation Efficiency (%)	Data Rate (Gbps)
DRA	25.4 (Res)*	$23.45 - 30.79 = 7.34$	-34.7	1.04	6.40	97.63	14.68
	28 (Opt.)*	$23.45 - 30.79 = 7.34$	-20.0	1.20	6.73	96.55	14.68
	34.6 (Res)*	$31.72 - 35.74 = 4.04$	-32.2	1.05	5.88	90.26	8.08
	38 (Res)*	$36.3 - 39.60 = 3.30$	-33.5	1.04	7.04	91.62	6.6
MPA	28 (Res)*	$27.41 - 28.9 = 1.49$	-23.6	1.14	5.41	90.33	2.98
	38 (Res)*	$37.55 - 38.56 = 1.01$	-27.1	1.09	4.89	84.32	2.02

(Res)* and Opt.* denote resonance and operating frequency, respectively.

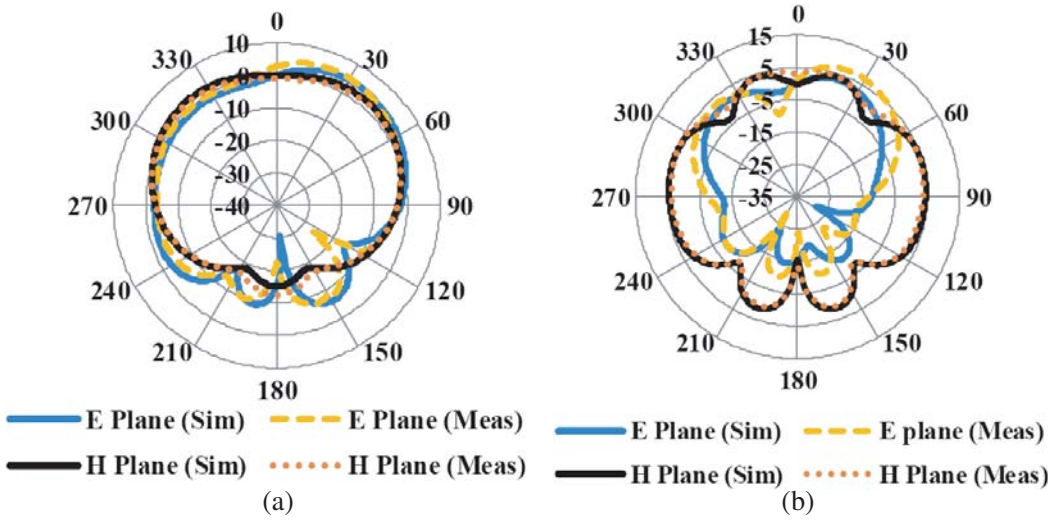

Figure 15. Radiation Pattern in E and H-plane at (a) 28 GHz and (b) 38 GHz of the proposed rectangular dual band patch antenna.

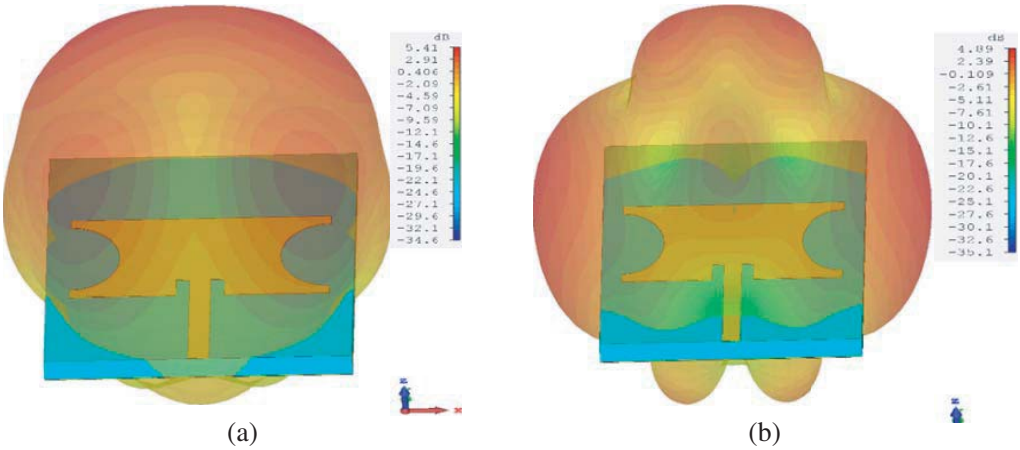

Figure 16. 3D view of gain plots at (a) 28 GHz and (b) 38 GHz of the proposed rectangular dual band patch antenna.

5. CONCLUSIONS AND FUTURE WORK

In this research work, a novel multiband rectangular dielectric resonator antenna for a future 5G wireless communication system, having stacked radiator with semi-circular slots etched on the left and right sides of upper radiator is designed. Till now, no such a compact size novel multiband dielectric resonator antenna with outstanding results developed in this work for future 5G communication system has been reported in literature. Furthermore, semi-elliptical slots rectangular microstrip patch antenna of the same dimensions for the purpose of comparison is designed. Parametric study is performed in order to achieve optimum designed values for the developed antennas. The developed dielectric antenna resonates at 25.4, 34.6, and 38 GHz with 7.34, 4.04, and 3.30 GHz of wide impedance bandwidths covering the targeted 5G, 28, and 38 GHz bands, having a good return loss of −34.7, −31.8, and −33.5 dB, respectively. Further, the designed dielectric antenna gives maximum radiation efficiency of 97.63%, with overall radiation efficiency greater than 90%, and the maximum gain of 7.6 dBi is also noted.

On the other hand, the proposed microstrip antenna resonates at 28 and 38 GHz with 1.49 and

1.01 GHz of moderate impedance bandwidth, having −23.6 and −27.1 dB of satisfactory return loss. Further, the proposed patch antenna gives the maximum radiation efficiency of 90.33% at 28 GHz, with overall radiation efficiency greater than 84%, and moderate gain of 5.45 dBi is also noted. Both the proposed antennas have nearly omnidirectional radiation patterns at resonance frequencies, with VSWR less than 2. Comparative study of the two proposed antennas regarding radiation efficiency, return loss, gain, data rate, and impedance bandwidth is done which evidently shows that the performance of DRA over MPA at millimeter wave is very good. Radiation parameters (gain) can be enhanced using array technique or by using novel Metasurfaces or Frequency Selective Surfaces (FSS) which can be integrated with the developed designs as superstrate or reflector. Important aspect of the 5G millimeter-wave antenna is to use it for beam steering purpose, so the proposed designs can be used for beam scanning purpose. Also, both the designed antennas can be converted into MIMO applications by applying the underlying theory.

REFERENCES

1. Commission of the European Communities, Staff Working Document, "Exploiting the employment potential of ICTs," Apr. 2012.
2. Wang, C.-X., F. Haider, X. Gao, X.-H. You, Y. Yang, D. Yuan, H. M. Ggoune, H. Haas, S. Fletcher, and E. Hepsaydir, "Cellular architecture and key technologies for 5G wireless communication networks," *IEEE Communications Magazine*, Vol. 52, No. 2, 122–130, Feb. 2014.
3. Ying, Z., "Antennas in cellular phones for mobile communications," *Proceedings of the IEEE*, Vol. 100, No. 7, 2286–2296, Jul. 2012.
4. Wang, C.-X., F. Haider, X. Gao, X.-H. You, Y. Yang, D. Yuan, H. Aggoune, H. Haas, S. Fletcher, and E. Hepsaydir, "Cellular architecture and key technologies for 5G wireless communication networks," *Communications Magazine*, Vol. 52, No. 2, 122, 130, IEEE, Feb. 2014.
5. Elkashlan, M., T. Q. Duong, and H.-H. Chen, "Millimeter-wave communications for 5G: Fundamentals: Part I [Guest Editorial]," *IEEE Communications Magazine*, Vol. 52, No. 9, 52–54, 2014.
6. Ali, M. M. M., O. Haraz, S. Alshebeili, and A. R. Sebak, "Broadband printed slot antenna for the fifth generation (5G) mobile and wireless communications," *17th International Symposium on Antenna Technology and Applied Electromagnetics (ANTEM)*, 1–2, Montreal, QC, 2016.
7. Parchin, N. O., M. Shen, and G. F. Pedersen, "End-fire phased array 5G antenna design using leaf-shaped bow-tie elements for 28/38 GHz MIMO applications," *IEEE International Conference on Ubiquitous Wireless Broadband (ICUWB)*, 1–4, Nanjing, 2016.
8. El-Bacha, A. and R. Sarkis, "Design of tilted taper slot antenna for 5G base station antenna circular array," *2016 IEEE Middle East Conference on Antennas and Propagation (MECAP)*, 1–4, Beirut, 2016.
9. Hong, W., K. H. Baek, Y. Lee, Y. Kim, and S. T. Ko, "Study and prototyping of practically large-scale mm Wave antenna systems for 5G cellular devices," *IEEE Communications Magazine*, Vol. 52, No. 9, 63–69, Sep. 2014.
10. Al-Falajy, N. and O. Y. K. Alani, "Design considerations of ultra dense 5G network in millimeter wave band," *2017 Ninth International Conference on Ubiquitous and Future Networks (ICUFN)*, 141–146, 2017.
11. Outerelo, D. A., A. V. Alejos, M. G. Sanchez, and M. V. Isasa, "Microstrip antenna for 5G broadband communication: Overview of design issues," *2015 IEEEinternational Symposium on Antennas and Propagation & USNC/URSI National Radio Science Meeting*, 2443–2444, 2015.
12. Ahmad, W. and W. T. Khan, "Small form factor dual band (28/38 GHz) PIFA antenna for 5G applications," *2017 IEEE MTTS International Conference on micromaves for Intelligent Mobility (ICMIM)*, 21–24, 2017.
13. Wu, T.-Y. and T. Chang, "Interference reduction by millimeter wave technology for 5G based green communications," *IEEE Journals & Magazines*, Vol. 4, 10228–10234, 2016.

14. Rouy, P., R. K, Vishwakarma, A. Jain, and R. Singh, "Multiband millimeter wave antenna array for 5G communication," *2016 International Conference on Emerging Trends in Electrical Electronics & Sustainable Energy Systems (ICETEESES)*, 102–105, 2016.
15. Chen, X.-P., K. Wu, L. Han, and F. He, "Low-cost high planar antenna array for 60-GHz band applications," *IEEE Transactions on Antennas and Propagation*, Vol. 58, No. 6, 2126–2129, Jun. 2010.
16. Biglarbegian, B., M. Fakharzadeh, D. Busuioc, M.-R. N. Ahmadi, and S. S. Naeini, "Optimized micro strip antenna arrays for emerging millimeter wave wireless applications," *IEEE Transactions on Antennas and Propagation*, Vol. 59, No. 5, 1742–1747, May 2011.
17. Wang, L., Y.-X. Guo, and W.-X. Sheng, "Wideband high-gain 60-GHz LTCCL probe patch antenna array with a soft surface," *IEEE Transactions on Antennas and Propagation*, Vol. 61, No. 4, 1802–1809, Apr. 2013.
18. Li, M. and K.-M. Luk, "Low-cost wideband micro strip antenna array for 60-GHz applications," *IEEE Transactions on Antennas and Propagation*, Vol. 62, No. 6, 3012–3018, Jun. 2014.
19. Balanis, C. A., *Antenna Theory Analysis and Design*, Wiley & Sons Ltd, New Jersy, 2005.
20. Huang, Y. and K. Boyle, *Antennas from Theory to Practice*, Wiley & Sons Ltd, West Sussex, 2008.
21. Khan, M., S. U. Rahman, M. K. Khan, and M. Saleem, "A dual notched band printed monopole antenna for ultra-wide band applications," *2016 Progress In Electromagnetic Research Symposium (PIERS)*, Shanghai, China, Aug. 8–11, 2016.
22. Rahman, S. U., M. I. Khan, N. Akhtar, and F. Murad, "Planar dipole antenna for tri-band PCS and WLAN communications," *Progress In Electromagnetic Research Symposium (PIERS)*, Shanghai, China, Aug. 8–11, 2016.
23. Ali, M. M. M. and A.-R. Sebak, "Dual band (28/38 GHz) CPW slot directive antenna for future 5G cellular applications," *2016 IEEE International Symposium on Antennas and Propagation & USNC/URSI National Radio Science Meeting*, 2016.
24. Saini, J. and S. K. Agarwal, "Design a single band microstrip patch antenna at 60 GHz millimeter wave for 5G applications," *2017 International Conference on Computer, Communications and Electronics (Comptelix)*, 227–230, IEEE Conference Publications, 2017.
25. Haraz, O. M., A. Elboushi, S. A. Alshebeili, and A. Sebak, "Dense dielectric patch array antenna with improved radiation characteristics using EBG ground structure and dielectric superstrate for future 5G cellular networks," *Access*, Vol. 2, 909, 913, IEEE, 2014.
26. Haraz, O. M., A. Elboushi, and A.-R. Sebak, "New dense dielectric patch array antenna for future 5G short-range communications," *The 16th International Symposium on Antenna Technology and Applied Electromagnetics (ANTEM 2014)*, Victoria, Canada, Jul. 13–17, 2014.
27. Ali, M. M. M., O. M. Haraz, S. Alshebeili, and A.-R. Sebak, "Design of broadband and dual-band printed slot antennas for the fifth generation (5G) mobile and wireless communications," *32nd National Radio Science Conference NRSC 2015*, Egypt, Oct. 6, 2015.
28. Petosa, A., A. Ittipiboon, Y. M. M. Antar, and D. Roscoe, "Recent advances in dielectric resonator antenna technology," *IEEE Antennas and Propagation Magazine*, Vol. 40, No. 3, 35–48, Jun. 1998.
29. Diao, Y., M. Su, Y. Liu , S. Li, and W. Wang, "Compact and multiband dielectric resonator antenna for mobile terminals," *IEEE International Symposium on Antennas and Propagation & USNC/URSI National Radio Science Meeting*, Jul. 2015.
30. Embong, N. and M. F. Mansor, "Multiband Dielectric Resonator Antenna (DRA) for Long Term Evolution Advanced (LTE-A) handheld devices," *International Conference on Space Science and Communication (IconSpace)*, Aug. 2015.
31. Jamaluddin, M. H., N. A. Mohammad, and S. Z. Naqiyah, "Size reduction of MIMO dielectric resonator antenna for LTE application," *IEEE Asia-Pacific Conference on Applied Electromagnetics (APACE)*, Dec. 2016.
32. Sher, C., Z. Chen, J. Yu, Y. Yao, L. Qi, and X. Chen, "A gain enhanced dielectric resonator antenna covering 62–78 GHz band for 5G," *International Conference on Microwave and Millimeter Wave Technology (ICMMT)*, May 2018.

33. Sharma, A., A. Sarkar, M. Adhikary, A. Biswas, and M. J. Akhtar, "SIW fed MIMO DRA for future 5G applications," *IEEE International Symposium on Antennas and Propagation & USNC/URSI National Radio Science Meeting*, Jul. 2017.
34. Ashikin Jaafar, N., M. H. Jamaluddin, J. Nasir, and N. M. Noor, "H-shaped dielectric resonator antenna for future 5G application," *IEEE International RF and Microwave Conference (RFM 2015)*, 14–16, Dec. 2015.
35. Perron, A., T. A. Denidni, and A.-R. Sebak, "High-gain hybriddielectric resonator antenna for millimeter-wave applications: Design and implementation," *IEEE Transactions on Antennas and Propagation*, Vol. 57, No. 10, 2882–2892, 2009.
36. Erfani, E., T. Denidni, S. Tatu, and M. Niroo-Jazi, "A broadband and high gain millimeter-wave hybrid dielectric resonator antenna," *Proceedings of the 17th International Symposium on Antenna Technology and Applied Electromagnetics (ANTEM'16)*, 1–2, IEEE, Montreal, Canada, Jul. 2016.
37. Lai, Q., C. Fumeaux, W. Hong, and R. Vahldieck, "60 GHz aperture-coupled dielectric resonator antennas fed by a halfmode substrate integrated waveguide," *IEEE Transactions on Antennas and Propagation*, Vol. 58, No. 6, 1856–1864, 2010.
38. Coulibaly, Y., M. Nedil, I. Ben Mabrouk, L. Talbi, and T. A. Denidni, "High gain rectangular dielectric resonator for broadband millimeter-waves underground communications," *Proceedings of the 24th Canadian Conference on Electrical and Computer Engineering (CCECE '11)*, 001088–001091, IEEE, Ontario, Canada, May 2011.
39. Coulibaly, Y., M. Nedil, L. Talbi, and T. A. Denidni, "Design of high gain and broadband antennas at 60 GHz for underground communications systems," *International Journal of Antennas and Propagation*, Vol. 2012, Article ID 386846, 7 pages, 2012.
40. Al-Hasan, M. J., T. A. Denidni, and A. R. Sebak, "Millimeter-wave EBG-based aperture-coupled dielectric resonator antenna," *IEEE Transactions on Antennas and Propagation*, Vol. 61, No. 8, 4354–4357, 2013.
41. Karimian, R., A. Kesavan, M. Nedil, and T. A. Denidni, "Low mutual coupling 60-GHz MIMO antenna system with frequency selective surface wall," *IEEE Antennas and Wireless Propagation Letters*, 2016.
42. Bijumon, P. V., Y. M. M. Antar, A. P. Freundorfer, and M. Sayer, "Integrated dielectric resonator antennas for system on-chip applications," *Proceedings of the International Conference on Microelectronics (ICM '07)*, 275–278, IEEE, Cairo, Egypt, Dec. 2007.
43. Allabouche, K., V. Bobrovs, F. Fererro, L. Lizzi, J.-M. Ribero, N. El Amrani El Idrissi, M. Jorio, and M. Elbakali, "Multiband rectangular dielectric resonator antenna for 5G applications," *International Conference on Wireless Technologies, Embedded and Intelligent Systems (WITS)*, 2017.
44. McAllister, M. W., S. A. Long, and G. L. Conway, "Rectangular dielectric resonator antenna," *Proceedings of the International Symposium Digest — Antennas and Propagation*, Vol. 21, 696–699, May 1983.
45. Leung, K. W., K. M. Luk, K. Y. A. Lai, and D. Lin, "Theory and experiment of a coaxial probe fed hemispherical dielectric resonator antenna," *IEEE Transactions on Antennas and Propagation*, Vol. 41, No. 10, 1390–1398, 1993.